

## PAPER

[View Article Online](#)  
[View Journal](#) | [View Issue](#)Cite this: *Nanoscale Adv.*, 2022, 4, 1545

## Domain wall motion driven by a wide range of current in coupled soft/hard ferromagnetic nanowires

Ziyang Yu,<sup>a</sup> Bin Gong,<sup>a</sup> Lun Xiong,<sup>a\*</sup> Xinran Du,<sup>b</sup> Chenhuinan Wei,<sup>b</sup> Rui Xiong,<sup>c</sup> Zhihong Lu<sup>d</sup> and Yue Zhang<sup>e\*</sup>

Racetrack memory with the advantages of small size and high reading speed is proposed based on current-induced domain wall (DW) motion in a ferromagnetic (FM) nanowire. Walker breakdown that restricts the enhancement of DW velocity in a single FM nanowire can be depressed by inter-wire magnetostatic coupling in a double FM nanowire system. However, this magnetostatic coupling also limits the working current density in a small range. In the present work, based on micromagnetic calculation, we have found that when there is a moderate difference of magnetic anisotropy constant between two FM nanowires, the critical current density for triggering the DW motion can be reduced while that for breaking the inter-wire coupling can be enhanced significantly to a magnitude of  $10^{13}$  A m<sup>-2</sup>, which is far above the working current density in current electronic devices. The manipulation of working current density is relevant to the modification of DW structure and inter-wire magnetostatic coupling due to the difference of the anisotropy constants between the two nanowires and paves a way to develop racetrack memory that can work in a wide range of current.

Received 5th July 2021  
Accepted 15th January 2022

DOI: 10.1039/d1na00540e

[rsc.li/nanoscale-advances](http://rsc.li/nanoscale-advances)

## Introduction

In racetrack memory that was proposed by Prof. Stuart S. P. Parkin of IBM in 2008,<sup>1</sup> digital information is stored in an array of magnetic domains in a nanowire of ferromagnetic metal (FM), and the domain wall (DW) that separates the neighboring domains is able to be driven by injecting an electrical current due to the spin-transfer torque (STT) effect.<sup>2–4</sup> When compared to a traditional hard disc driver, the racetrack memory device exhibits advantages of small size and high reading speed. Therefore, the current induced DW motion (CIDWM) in an FM nanowire has been widely investigated in experiments and in theory.<sup>5–12</sup>

In CIDWM, the stability of DW structure depends on current density. When the current density exceeds a critical value, the magnetic moments in the DW precess, and the DW motion slows down. This is the so-called Walker breakdown.<sup>8,13–15</sup>

Depression of the Walker breakdown results in DW motion at a high velocity with a stable DW structure. In 2015, Purnama *et al.* found that in an FM/insulator/FM sandwiched nanowire with perpendicular magnetic anisotropy (PMA), the magnetostatic coupling between the DWs in the neighboring FM nanowires provides a closed magnetic line of force that stabilizes the DW structure and depresses the Walker breakdown.<sup>16</sup> The depression of Walker breakdown by inter-wire magnetostatic coupling has also been observed experimentally very recently.<sup>17</sup> However, the inter-wire magnetostatic coupling also restricts the range of working current, and the DW can only be induced to move with the current density between two critical values. One is the smallest current density ( $J_a$ ) to overcome the pinning due to the inter-wire magnetostatic coupling.<sup>16</sup> Lowering  $J_a$  reduces dissipation. On the other hand, when the current density is higher than another critical value ( $J_b$ ), the two DWs are decoupled. When the current density is between  $J_a$  and  $J_b$ , the Walker breakdown is depressed.<sup>16</sup> Therefore, a low  $J_a$  with a high  $J_b$  is expectable in such a double FM nanowire system. However, in a sandwiched multilayer composed of two FM nanowires with identical parameters, lowering  $J_a$  and enhancing  $J_b$  at the same time seems not easy. This is because the magnetostatic coupling acting on the two DWs is the same, and they become stronger or weaker together. As a result, the range of current density for the synchronization of DW motion is fixed in a small range.

In the present work, we have found that the small difference of the magnetic anisotropy constant between the two nanowires

<sup>a</sup>Hubei Key Laboratory of Optical Information and Pattern Recognition, School of Optical Information and Energy Engineering, Wuhan Institute of Technology, Wuhan 430205, P. R. China. E-mail: [xionglin@wit.edu.cn](mailto:xionglin@wit.edu.cn)

<sup>b</sup>Hubei Provincial Key Laboratory of Green Materials for Light Industry, Hubei University of Technology, Wuhan 430068, China

<sup>c</sup>Key Laboratory of Artificial Micro- and Nano-structures of Ministry of Education, School of Physics and Technology, Wuhan University, Wuhan 430072, China

<sup>d</sup>The State Key Laboratory of Refractories and Metallurgy, School of Materials and Metallurgy, Wuhan University of Science and Technology, Wuhan 430081, China

<sup>e</sup>School of Optical and Electronic Information, Huazhong University of Science and Technology, Wuhan, 430074, China. E-mail: [yue-zhang@hust.edu.cn](mailto:yue-zhang@hust.edu.cn)

is able to reduce  $J_a$  and enhance  $J_b$  at the same time. As a result, the gap between  $J_a$  and  $J_b$  is significantly enlarged, and  $J_b$  becomes even higher than  $10^{13} \text{ A m}^{-2}$ , which is far beyond the current density that can be injected in current electronic devices.

## Methods

The CIDWM is simulated using the micromagnetic simulation software named Object-Oriented Micromagnetic Framework (OOMMF). In the simulation, we consider the CIDWM in a double FM nanowire system with PMA, and the magnetic

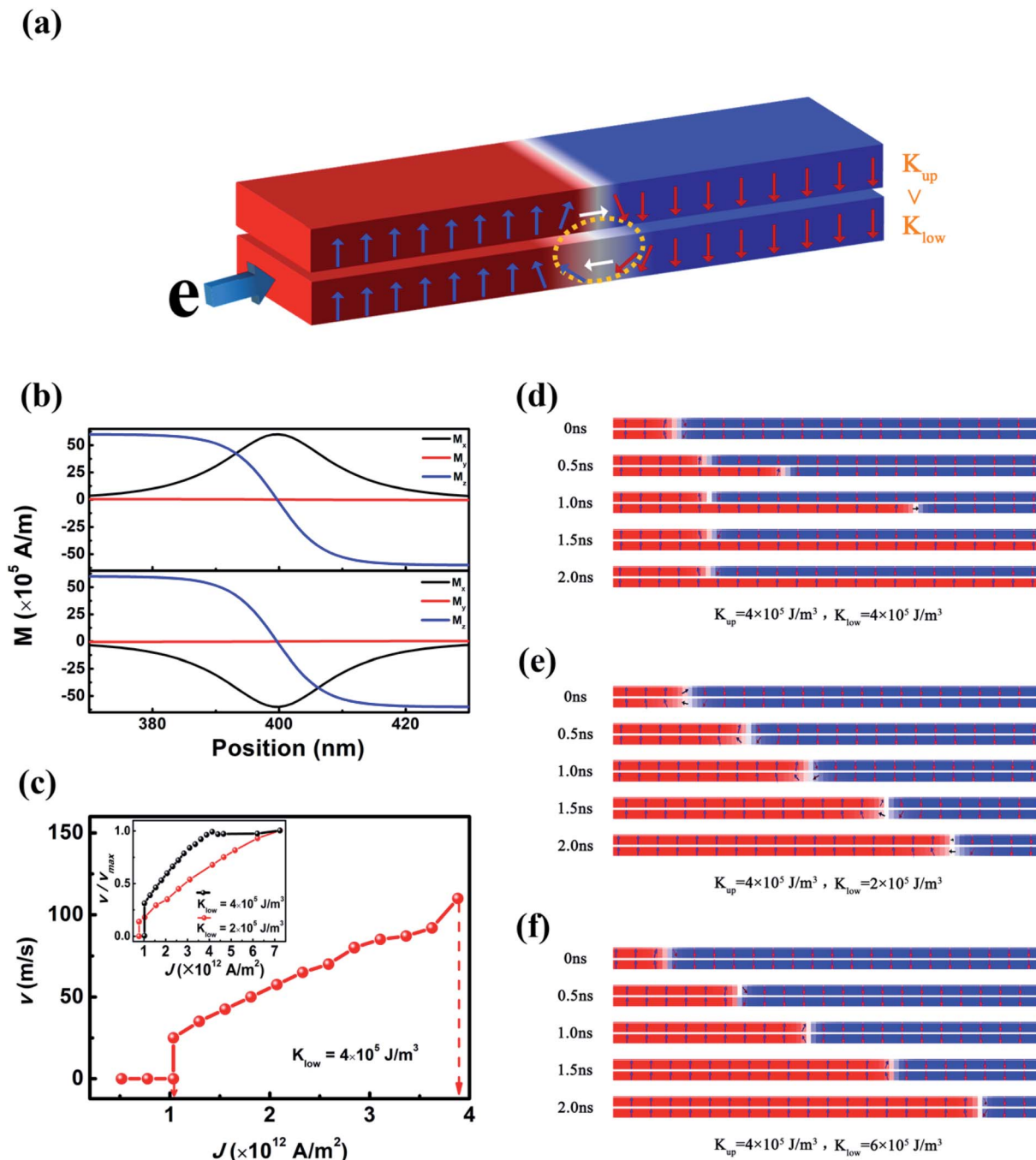


**Fig. 1** (a) Model: the double FM nanowire system composed of two FM nanowires with distinct magnetic anisotropy constants (the lower DW is induced to move under the injection of current, and the upper one is also dragged to move by the interlayer magnetostatic coupling); (b)  $x$ ,  $y$ , and  $z$  components of magnetization near the centre of the DW in the two nanowires with  $K_l = K_u = 4 \times 10^5 \text{ J m}^{-3}$ ; (c) average velocity for the lower DW in the double nanowire system with  $K_l = K_u = 4 \times 10^5 \text{ J m}^{-3}$  as a function of current density ( $J$ ) (inset: comparison of the normalized velocity for the lower DW in the double nanowire system with  $K_l = K_u = 4 \times 10^5 \text{ J m}^{-3}$  and that with  $K_l = 2 \times 10^5 \text{ J m}^{-3}$  and  $K_u = 4 \times 10^5 \text{ J m}^{-3}$ ); (d–f) snapshots of DW motion under  $J = 7.5 \times 10^{12} \text{ A m}^{-2}$  for  $K_l = K_u = 4 \times 10^5 \text{ J m}^{-3}$ ,  $K_l = 2 \times 10^5 \text{ J m}^{-3}$  and  $K_u = 4 \times 10^5 \text{ J m}^{-3}$ , and  $K_l = 6 \times 10^5 \text{ J m}^{-3}$  and  $K_u = 4 \times 10^5 \text{ J m}^{-3}$ .



anisotropy constants of the upper ( $K_u$ ) and lower ( $K_l$ ) nanowires are different (Fig. 1(a)). The interfacial Dzyaloshinskii–Moriya interaction (DMI) is also taken into account since it usually exists in an ultrathin FM film with PMA and contributes to stabilizing the Néel-type DW structure.<sup>17,18</sup> The current is injected into the lower nanowire, in which the DW is driven due to the STT effect. Because of the inter-layer magnetostatic coupling, the DW in the upper one is also dragged to move to reduce the demagnetization energy till the current density is above  $J_b$ .

The simulation is based on resolving the Landau–Lifshitz–Gilbert (LLG) equation containing the STT terms:<sup>8</sup>

$$\frac{\partial \vec{m}}{\partial t} = -\gamma \vec{m} \times \vec{H}_{\text{eff}} + \alpha \vec{m} \times \frac{\partial \vec{m}}{\partial t} + u \vec{m} \times \left( \vec{m} \times \frac{\partial \vec{m}}{\partial x} \right) + \beta u \vec{m} \times \frac{\partial \vec{m}}{\partial x} \quad (1)$$

In eqn (1), the parameters  $\vec{m}$ ,  $t$ , and  $\gamma$  represent the unit vector for the orientation of magnetic moment, time, and the absolute value of gyromagnetic ratio. The first and second terms at the right side of eqn (1) contribute to the torque from the effective magnetic field  $\vec{H}_{\text{eff}}$  and Gilbert damping with the damping coefficient  $\alpha = 0.01$ , respectively. The third and fourth terms are the adiabatic and non-adiabatic STT with the coefficient  $\beta = 0.04$ ,<sup>16</sup> respectively. Here  $\beta$  is significantly larger than

$\alpha$ , which will lead to the STT-induced Walker breakdown under a small  $J$ .<sup>8</sup>  $u$  is the velocity of an electron:  $u = \frac{JPg\mu_B}{2eM_s}$ , where  $J$  is the current density,  $P$  is the polarization rate ( $P = 0.7$ ),  $g$  is the Landé factor,  $\mu_B$  is the Bohr magneton, and  $e$  is the electron charge.

The model and parameters are as follows: the length and width of the nanowire are 5000 nm and 40 nm, respectively. The lower nanowire and the upper one share the same thickness (6 nm), and the inter-wire distance is 2 nm. The cell dimensions are 5 nm  $\times$  5 nm  $\times$  2 nm. The saturation magnetization ( $M_s$ ) is  $6 \times 10^5$  A m<sup>-1</sup>. The exchange stiffness constant ( $A$ ) is  $1.3 \times 10^{-11}$  J m<sup>-1</sup>. The absolute value of the DMI constant ( $D$ ) is between 0 mJ m<sup>-2</sup> and 1 mJ m<sup>-2</sup>, and the signs of  $D$  of the two nanowires are opposite. The  $K_u$  is fixed as  $4 \times 10^5$  J m<sup>-3</sup>, and the  $K_l$  changes between  $2 \times 10^5$  J m<sup>-3</sup> and  $6 \times 10^5$  J m<sup>-3</sup>.

## Results and discussion

Initially, the Néel-type DWs are generated in the two nanowires (Fig. 1(b)). Because of their opposite chirality, a closed magnetic line of force can be generated between the two nanowires.<sup>16,17</sup> When both  $K_u$  and  $K_l$  are  $4 \times 10^5$  J m<sup>-3</sup>,  $J_a$  and  $J_b$  are  $0.9 \times 10^{12}$  A m<sup>-2</sup> and  $3.7 \times 10^{12}$  A m<sup>-2</sup>, respectively (Fig. 1(c)). When  $J$  is 7.5

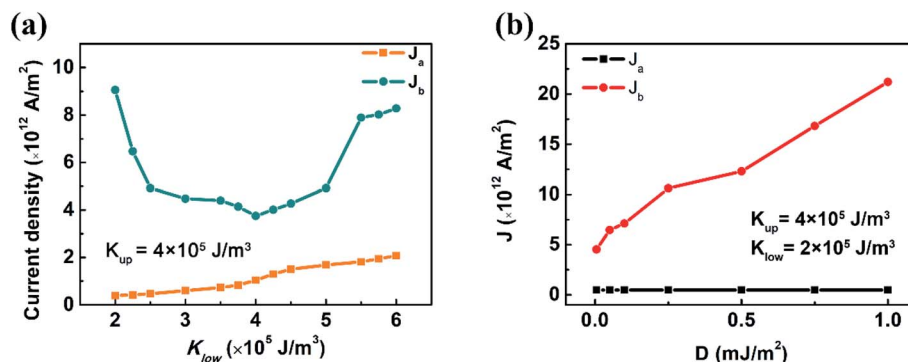


Fig. 2 Critical current density  $J_a$  and  $J_b$  as a function of (a) the anisotropy constant of the lower layer  $K_l$  ( $K_u$  is fixed at  $4 \times 10^5$  J m<sup>-3</sup>) and (b) DMI constant  $D$ .

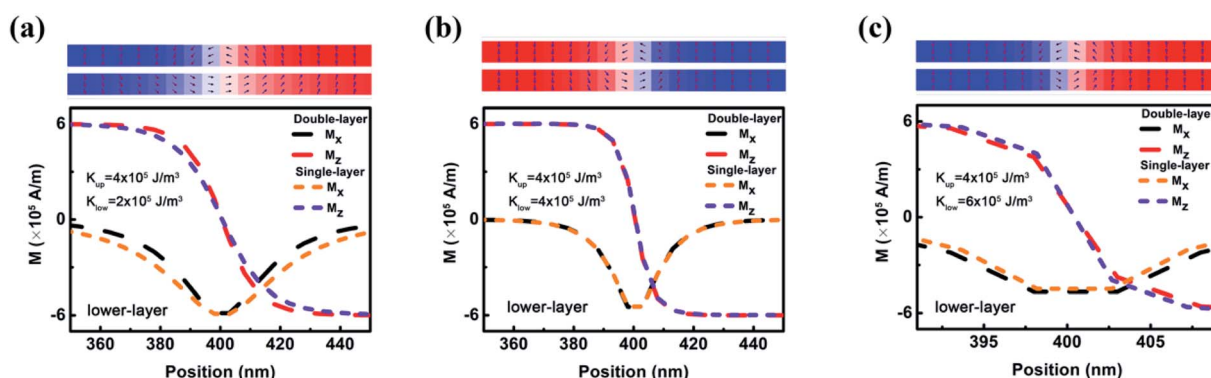


Fig. 3  $x$  and  $z$  components of magnetization near the centre of the lower DW in the double nanowire system with a fixed  $K_u$  ( $4 \times 10^5$  J m<sup>-3</sup>) and different  $K_l$  ((a)  $K_l = 2 \times 10^5$  J m<sup>-3</sup>, (b)  $K_l = 4 \times 10^5$  J m<sup>-3</sup>, and (c)  $K_l = 6 \times 10^5$  J m<sup>-3</sup>) and that in the single nanowire with the same  $K_l$ . The upper panels show the configuration of double nanowire magnetic moments in the range of position coordinates.



$\times 10^{12} \text{ A m}^{-2}$ , higher than this  $J_b$ , the lower DW is able to be driven by STT, but the upper DW is decoupled with the lower one (Fig. 1(d)). However, when  $K_1$  is  $2 \times 10^5 \text{ J m}^{-3}$  or  $6 \times 10^5 \text{ J m}^{-3}$ , the upper DW can still be dragged to move together with the lower one under the same  $J$  (Fig. 1(e) and (f)). This indicates that the small difference of the magnetic anisotropy constant between the two nanowires contributes to the enhancement of  $J_b$ . Additionally, when  $K_u = K_1 = 4 \times 10^5 \text{ J m}^{-3}$ , the increase of DW velocity is depressed when  $J$  exceeds  $J_b$ ,  $3.7 \times 10^{12} \text{ A m}^{-2}$ . Nevertheless, with  $K_1 = 2 \times 10^5 \text{ J m}^{-3}$ , the DW velocity keeps increasing when  $J$  is far beyond  $4 \times 10^{12} \text{ A m}^{-2}$ , indicating the

depression of Walker breakdown under a higher current (the inset figure of Fig. 1(c)). And the reversal time of magnetic moments is about 0.01 ns.

The variation of  $J_a$  and  $J_b$  with  $K_1$  ( $K_u$  is fixed at  $4 \times 10^5 \text{ J m}^{-3}$ ) is different (Fig. 2(a)). When  $K_1$  increases from  $2 \times 10^5 \text{ J m}^{-3}$  to  $6 \times 10^5 \text{ J m}^{-3}$ ,  $J_a$  increases monotonically from  $5 \times 10^{11} \text{ A m}^{-2}$  to around  $2 \times 10^{12} \text{ A m}^{-2}$ . However,  $J_b$  changes with  $K_1$  non-monotonically:  $J_b$  is close to  $1 \times 10^{13} \text{ A m}^{-2}$  when  $K_1$  is  $2 \times 10^5 \text{ J m}^{-3}$ . It decreases with increasing  $K_1$  and reaches the minimum value when  $K_1 = K_u$  and is enhanced again with further increase in  $K_1$ . When  $K_1$  and  $K_u$  are fixed at  $2 \times 10^5 \text{ J m}^{-3}$

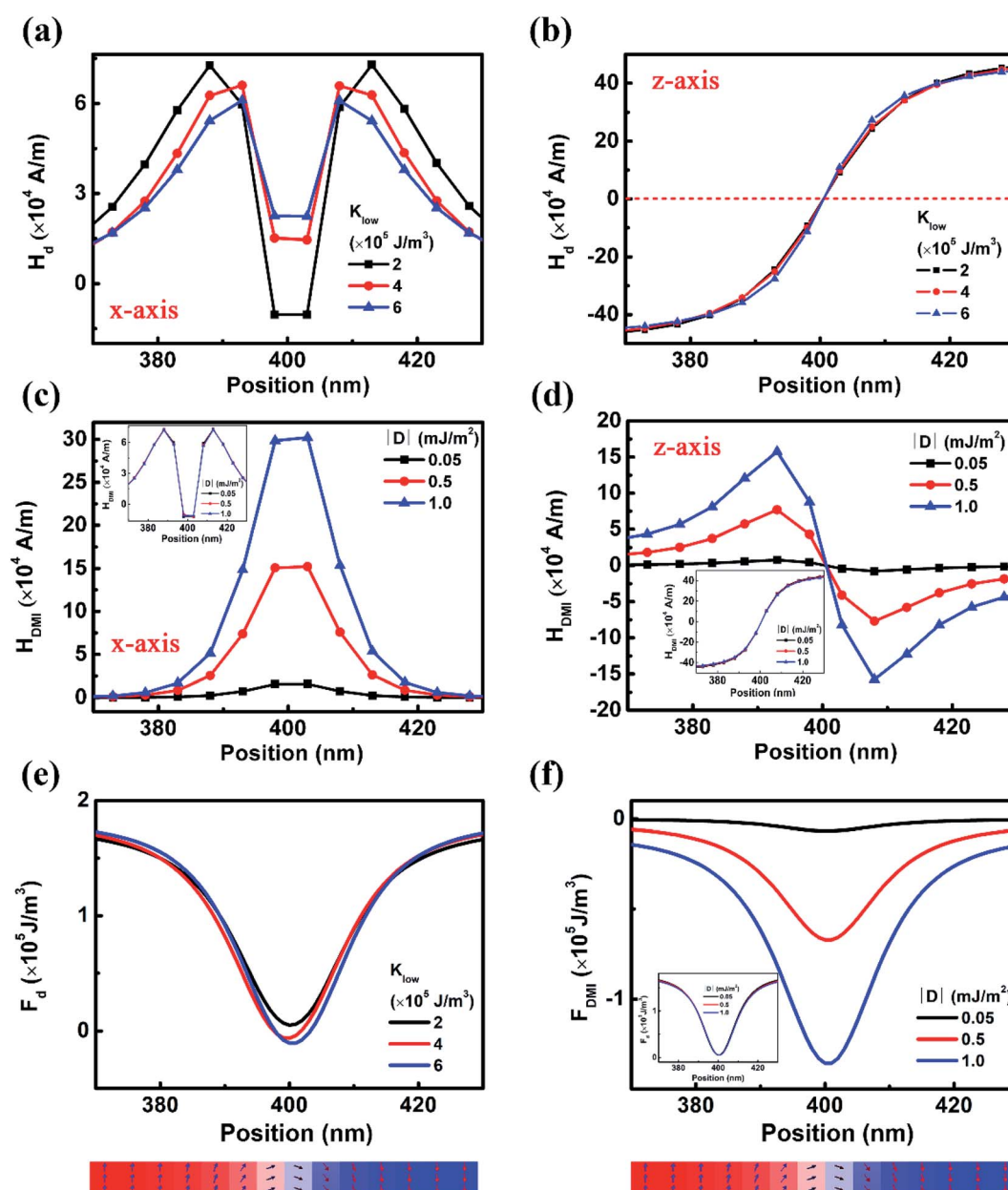


Fig. 4 (a) x and (b) z components of the demagnetizing field in the DW region with different  $K_1$ ; (c) x and (d) z components of the DMI effective field in the DW region with different  $D$  (inset: (c) x and (d) z components of the demagnetizing field with different  $D$ ); (e) density of demagnetizing energy in the DW region with different  $K_1$  and (f) energy density of DMI in the DW region with different  $D$  (inset: density of demagnetizing energy with different  $D$ ). The lower panels show the configuration of magnetic moments in the range of position coordinates as shown in (a) to (f).





and  $4 \times 10^5 \text{ J m}^{-3}$ ,  $J_b$  can be further modified by manipulating  $D$  (Fig. 2(b)). When  $D$  increases from  $0.05 \text{ mJ m}^{-2}$  to  $1 \text{ mJ m}^{-2}$ ,  $J_a$  does not change, but  $J_b$  keeps increasing to  $2 \times 10^{13} \text{ A m}^{-2}$ , which is far beyond the upper limit of electrical current density for current electronic devices. It is noticed that this  $D$  is reasonable in experiments for some heavy metal/FM multilayers such as Pt/Co.<sup>19,20</sup>

In theory, when  $\beta$  is larger than  $\alpha$ , the DW in a single FM nanowire is able to be driven if only the current density is higher than zero.<sup>8,16</sup> However, the inter-wire magnetostatic coupling in the double FM nanowire system pins the DW motion and results in a nonzero  $J_a$ .<sup>16</sup> When  $K_l$  is different from  $K_u$ , the inter-wire magnetostatic coupling may assist or hinder the motion of the lower DW, depending on the difference between  $K_l$  and  $K_u$ . As indicated in Fig. 3, the structure of the lower DW in the double-nanowire system is modified due to the magnetostatic coupling from the upper DW. When  $K_l$  is  $2 \times 10^5 \text{ J m}^{-3}$ , the lower DW in the double nanowire system is narrower than that in the single nanowire with the same parameters. This means that the magnetostatic coupling rotates the magnetic moments in the left part of the lower DW towards the  $+z$  axis. In the CIDWM, the DW is triggered to move to the right through the STT-driven rotation of the magnetic moments at the left of the DW towards the  $+z$  axis. Therefore, when  $K_l$  is  $2 \times 10^5 \text{ J m}^{-3}$ , the magnetostatic coupling assists this rotation of magnetic moments, and the DW is able to move under a weaker current. When  $K_l$  is  $6 \times 10^5 \text{ J m}^{-3}$ , higher than  $K_u$ , the situation is the opposite: the magnetostatic coupling from the upper DW widens the lower DW and hinders the rotation of magnetic moments.

To understand the non-monotonic variation of  $J_b$ , one needs to consider the variation of the magnetostatic coupling acting on the upper DW. This may be indirectly reflected from the demagnetizing field ( $H_d$ ) near the DW in the initial state. Because of the Néel-type DW structure, we only consider the  $H_d$  in the  $xz$  plane. The  $x$  and  $z$  components of  $H_d$  are extracted from the OOMMF. It is shown that changing  $K_l$  has a small effect on  $(H_d)_z$ , but changes  $(H_d)_x$  considerably. When  $K_l$  increases from  $2 \times 10^5 \text{ J m}^{-3}$  to  $6 \times 10^5 \text{ J m}^{-3}$ , the  $(H_d)_x$  near the centre of the DW is enhanced, while that near the DW edge decreases. This indicates that when  $K_l$  is low or high, a strong  $(H_d)_x$  assists the rotation of the magnetic moments either in the centre or at the edge of the DW. Since the DMI effective field is also in the  $xz$  plane, the changing of DMI also modifies the effective field for assisting/hindering the rotation of magnetic moments near the DW region. Both  $x$  and  $z$  components of the DMI effective field ( $(H_{\text{DMI}})_x$  and  $(H_{\text{DMI}})_z$ ) are enhanced with increasing  $D$  (Fig. 4(c) and (d)), but  $H_d$  does not change obviously (the inset figures in Fig. 4(c) and (d)). The increasing  $(H_{\text{DMI}})_z$  at the left edge of the DW assists the rotation of magnetic moments towards the  $+z$  direction, which makes it easy for the upper DW to move to the right and enhances  $J_b$ .

The non-monotonic changing of  $J_b$  may also be understood from the aspect of free energy density. When  $K_l = 2 \times 10^5 \text{ J m}^{-3}$ , the demagnetizing energy density ( $F_d$ ) throughout the upper DW region is higher than that for  $K_l = 4 \times 10^5 \text{ J m}^{-3}$ . When  $K_l = 6 \times 10^5 \text{ J m}^{-3}$ , the  $F_d$  at the left side of the upper DW is also

higher than that for  $K_l = 4 \times 10^5 \text{ J m}^{-3}$  (Fig. 4(e)). Therefore, in both cases, the magnetic moments at the left side of the upper DW have a higher demagnetizing energy, which increases the probability for the rotation and the DW motion to the right. On the other hand, the energy density of DMI near the DW region increases with increasing  $D$  (Fig. 4(f)), yet the changing of DMI has little impact on the  $F_d$  (the inset figure of Fig. 4(f)). This also confirms that in addition to demagnetizing field, DMI also contributes to the enhancement of  $J_b$ .

## Conclusion

In summary, in a coupled FM nanowire system, when the current is injected into the nanowire whose magnetic anisotropy constant is moderately lower than that of the other one, the DW can be triggered to move under a weaker current with a more stable magnetostatic coupling between the DWs in the two nanowires. This inter-layer magnetostatic coupling stabilizes the DW structure, depresses the Walker breakdown, and widens the range of current density for the DW motion. This paves a way to develop a novel racetrack memory device with low dissipation and high reading speed.

## Conflicts of interest

There are no conflicts to declare.

## Acknowledgements

The authors acknowledge financial support from the National Natural Science Foundation of China (No. 12104348, 51971098 and 11804211), the Major Research Plan of the National Natural Science Foundation of China (No. 91963207) and the Science and Technology Department of Hubei Province (No. 2019CFB435).

## References

- 1 S. Parkin, M. Hayashi and L. Thomas, *Science*, 2008, **320**, 190–194.
- 2 D. C. Ralph and M. D. Stiles, *J. Magn. Magn. Mater.*, 2008, **320**, 1190–1216.
- 3 S. Muehlbauer, B. Binz, F. Jonietz, C. Pfleiderer, A. Rosch, A. Neubauer, R. Georgii and P. Boeni, *Science*, 2009, **323**(5916), 915–919.
- 4 M. Yamanouchi, D. Chiba, F. Matsukura, T. Dietl and H. Ohno, *Phys. Rev. Lett.*, 2006, **96**, 79–92.
- 5 C. Adrian, *Science*, 2008, **320**, 166.
- 6 A. Brataas, A. D. Kent and H. Ohno, *Nat. Mater.*, 2012, **11**, 372.
- 7 L. M. Miron, T. Moore, H. Szambolics, L. D. Buda-Prejbeanu, S. Auffret, B. Rodmacq, S. Pizzini, J. Vogel, M. Bonfim and A. Schuhl, *Nat. Mater.*, 2011, **10**, 419–423.
- 8 A. Thiaville, Y. Nakatani, J. Miltat and Y. Suzuki, *Europhys. Lett.*, 2005, **69**, 990–996.



- 9 T. Koyama, D. Chiba, K. Ueda, K. Kondou, H. Tanigawa, S. Fukami, T. Suzuki, N. Ohshima, N. Ishiwata and Y. Nakatani, *Nat. Mater.*, 2011, **10**(3), 194–197.
- 10 Z. Li and S. Zhang, *Phys. Rev. B: Condens. Matter Mater. Phys.*, 2004, **70**, 2199–2208.
- 11 O. Boulle, J. G. Kimling, P. Warnicke, M. Klui and G. Faini, *Phys. Rev. Lett.*, 2008, **101**, 216601.
- 12 S. Krishnia and W. S. Lew, in *Emerging Non-volatile Memory Technologies*, Springer, 2021, pp. 103–147.
- 13 C. J. Slonczewski and, *J. Appl. Phys.*, 1991, **69**, 4590–4592.
- 14 N. L. Schryer and L. R. Walker, *J. Appl. Phys.*, 1974, **45**, 5406–5421.
- 15 J. Moon, J. Yoon, K. Kim, S.-H. Lee, D.-Y. Kim and S.-B. Choe, *Multiple Walker Breakdowns in Magnetic Multilayers*, 2021, preprint, DOI: 10.21203/rs.3.rs-775358/v1.
- 16 I. Purnama, I. S. Kerk, G. J. Lim and W. S. Lew, *Sci. Rep.*, 2015, **5**(1), 8754.
- 17 A. Hrabec, V. Krizakova, S. Pizzini, J. Sampaio, A. Thiaville, S. Rohart and J. Vogel, *Phys. Rev. Lett.*, 2018, **120**, 227204.227201–227204.227205.
- 18 S. Rohart and A. Thiaville, *Physics*, 2013, **88**, 1352–1355.
- 19 H. Yang, A. Thiaville, S. Rohart, A. Fert and M. Chshiev, *Phys. Rev. Lett.*, 2015, **115**, 267210.
- 20 W. Legrand, D. Maccariello, F. Ajejas, S. Collin, A. Vecchiola, K. Bouzehouane, N. Reyren, V. Cros and A. Fert, *Nat. Mater.*, 2020, **19**(1), 34–42.

